Intrinsic chlorine resistance of bacteria modulated by glutaminyl-tRNA biosynthesis in drinking water supply systems

Xiaocao Miao [a,b], Xue Han [a], Chenxu Liu [a], Xiaohui Bai [a,*]

[a] State Key Laboratory of Microbial Metabolism, Joint International Research Laboratory of Metabolic & Developmental Sciences, School of Life Sciences and Biotechnology, Shanghai Jiao Tong University, Shanghai, 200240, PR China
[b] State Key Laboratory of Oncogenes and Related Genes, Shanghai Cancer Institute, Ren Ji Hospital, School of Medicine, Shanghai Jiao Tong University, Shanghai, PR China

HIGHLIGHTS

- The dominant CRB interacted strongly to maintain basic metabolism.
- Glutaminyl-tRNA biosynthesis was the key metabolic pathway of CRB.
- The *GlnRS* overexpression strain showed a lower inactivation rate after chloramination.
- The chlorine resistance of bacteria can be modulated by *GlnRS* in DWSSs.

GRAPHICAL ABSTRACT

ARTICLE INFO

ABSTRACT

The existence of chlorine-resistant bacteria (CRB) in drinking water supply systems (DWSSs) results in significant challenges to the biological security of drinking water. However, little is known about the intrinsic chlorine-resistant molecular metabolic mechanism of bacteria in DWSSs. This research explored the microbial interactions and the key metabolic pathways that modulate the chlorine resistance of bacteria in full-scale chloraminated DWSSs. The dominant CRB, including *Bdellovibrio*, *Bradyrhizobium*, *Peredibacter*, *Sphingomonas*, and *Hydrogenophaga*, strongly interacted with each other to maintain basic metabolism. A total of 4.21% of the bacterial metabolic pathways were key and specific to chlorine-resistant bacteria. Glutaminyl-tRNA biosynthesis was the dominant metabolic pathway of CRB in the target DWSSs. After chloramine disinfection, the relative abundance of glutamate-tRNA ligase (*GlnRS*) and the related orthologous genes increased by 10.11% and 14.58%, respectively. The inactivation rate of the *GlnRS* overexpression strain (81.40%) was lower than that of the wild-type strain (90.11%) after exposure to chloramine. Meanwhile, the growth rate of the *GlnRS* overexpression strain was higher than that of the wild-type strain. Glutaminyl-tRNA biosynthesis can enhance chlorine resistance in DWSSs.
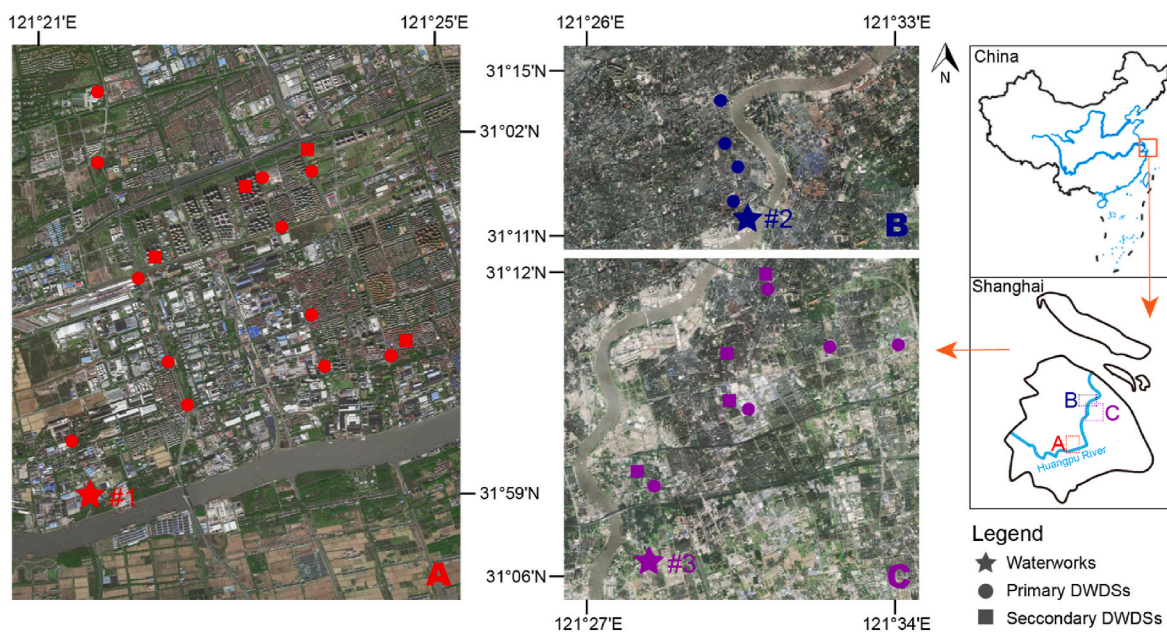
Fig. 1. Geographical locations of the sampling sites. Sampling locations were within three waterworks (#1, #2 and #3) and their respective DWDSs.

1. Introduction

Chlorine, a strong oxidant, is the most commonly used disinfectant in water treatment because of its effectiveness, ease of use, and low cost (Simões et al., 2010). Chlorine disinfection is usually the last process for water treatment, and the residual chlorine needs to be maintained until the terminal pipeline to control the growth of microorganisms during the transmission and distribution of drinking water in Shanghai, the largest international metropolis in China (Bai et al., 2015a,b; Douterelo et al., 2018). The use of disinfectants has imposed selective pressure and contributed greatly to the emergence of disinfectant-resistant microorganisms in water (Langsrud et al., 2003). Chlorine-resistant bacteria (CRB) are commonly defined as bacteria with high resistance to chlorine disinfection or bacteria that can survive or even regrow in water with residual chlorine (Luo et al., 2021). The World Health Organization proposed a method to evaluate the chlorine resistance of pathogenic microorganisms, which was based on the survival time of microorganisms at conventional disinfection doses; 99% inactivation at 20 °C (low <1 min; moderate 1–30 min and high >30 min) (WHO, 2011). The existence of CRB (i.e., pathogenic, odor-producing, or corrosion-resistant bacteria) not only increases the difficulty of microbial control in effluent water but also causes significant challenges to the biological security of drinking water in drinking water supply systems (DWSSs) (Roy and Ghosh, 2017).

Bacterial chlorine resistance mechanisms include biochemical structural mechanisms (external resistance) and genetic pathway mechanisms (internal resistance). Four kinds of cellular permeability barriers (i.e., extracellular polymeric substances, cell wall, cell membrane, and spore coats) against chlorine can provide chlorine resistance (Luo et al., 2021). Gram-positive (G+) bacteria have stronger chlorine resistance than Gram-negative (G−) bacteria because of their thicker cell walls (Mir et al., 1997). *Mycobacterium* relies on waxy substances that enhance hydrophobicity and barrier function to resist disinfectants (Furuhata et al., 2014). The intracellular spore of *Bacillus* has a thick multilayer structure with low water content, enhancing chlorine resistance of *Bacillus* (Ortega Morente et al., 2013). The extracellular polymeric substance secreted by *Sphingomonas* can promote the chlorine resistance of *Sphingomonas* (Bereschenko et al., 2010). The above resistant effects are determined by internal resistance (Luo et al., 2021).

Internal intrinsic resistance is the resistance determined by genetic materials. Different genera of bacteria have different resistance levels and mechanisms (Luo et al., 2021). Bacteria exhibit an oxidizing stress response by producing oxidant-degrading and repair enzymes to become more resistant to deleterious factors. A variety of defense genes have been characterized in the model strain *E. coli*, encoding various superoxide dismutases, catalysts, alkyl hydroperoxide reductases, glutathione reductases, and DNA repair enzymes (Cloete, 2003). Regulatory genes have been characterized in *E. coli*, i.e., *soxR*, which determines intracellular redox potential and activates the stress response when cells are exposed to oxidizing agents (Demple, 1996). Research on bacterial chlorine resistance mechanisms has mainly focused on external resistance. There have been a few studies on the internal resistance mechanisms of CRB based on model strains (Cloete, 2003; Luo et al., 2021). However, whether there exists a genetic mechanism for CRB and what the genetic mechanism for CRB in the complex and real drinking water supply systems remains unclear.

This research aimed to explore the intrinsic molecular mechanism of CRB in response to chlorine oxidation stress based on the metabolic pathway of microorganisms in full-scale chloraminated DWSSs. We obtained culturable CRB by isolation from DWSSs and the composition of nonculturable CRB by high-throughput sequencing. The chlorine resistance genes of CRB were screened by comparing the interaction mode and metabolic pathway of bacteria in high- and low-chlorinated water. Finally, an overexpression strain with a chlorine resistance gene was constructed, and the chlorine resistance phenotype was verified.

2. Materials and methods

2.1. Drinking water supply systems and sampling

This research was conducted in three full-scale drinking water treatment systems (DWTSs) and their drinking water distribution systems (DWDSs) in Shanghai, China (Fig. 1). One of the DWTSs (#1) receives water from the Jinze Reservoir, and the remaining two DWTSs (#2 and #3) receive water from the Qingcaosha Reservoir sourced from the Yangtze River. Water samples collected in DWTS #1 included raw water, sedimentation, sand filtration, ozone oxidation, biological activated carbon (BAC) filtration, and chloramine disinfection (effluent water) samples. Because the treatment process of DWTS 3# added

Table 1

Composition of culturable CRB isolated from the water supply systems.

Order	Family	Genus	Colony number[a]	Proportion
Rhizobiales	Methylobacteriaceae	*Methylobacterium*	5	4.90%
Corynebacteriales	Mycobacteriaceae	*Mycobacterium*	18	17.65%
Sphingomonadales	Sphingomonadaceae	*Sphingomonas*	33	32.35%
Rhizobiales	Xanthobacteraceae	Bradyrhizobium	46	45.10%

[a] The colony number was based on 0.2 mL of drinking water sample.

ultraviolet (UV) treatment after BAC filtration, water samples collected in DWTS 3# included additional post UV samples. Twenty liters of water were collected for microbial analysis and DNA extraction after a few minutes of flushing. All samples were transported to the laboratory on ice and processed within 12 h and they were collected from May 2018 to Oct 2020. The total chlorine and temperature measurements were performed in situ.

2.2. CRB isolation and identification

Heterotrophic plate count (HPC) was performed with R2 agar (R2A), and the plates were incubated at 28 °C for 7 d (El-Chakhtoura et al., 2015). All measurements were performed in triplicate. HPC bacteria isolated from water samples with total chlorine concentrations greater than 0.5 mg/L were identified as CRB (Luo et al., 2021). The spread plate method was used for bacterial purification.

The DNA extraction for the selected bacteria was performed by using a boiling method as previously described (Bai et al., 2015a,b). 16S rDNA sequencing using the universal primers 27F and 1492R was used to identify the bacterial isolates (Cox, C.R. and M.S. Gilmore, 2007). The amplified nucleotide sequences were used for NCBI BLAST searches (http://www.ncbi.nlm.nih.gov).

2.3. Cloning and transformation of the GlnRS gene

Luria–Bertani (LB) media and R2A media were used as the culture media. If necessary, kanamycin (50 mg/L for *E. coli*) and ampicillin were supplemented. Gene glutamate-tRNA ligase (*GlnRS*, 1503 bp) from *Sphingomonas paucimobilis,* which was obtained from tap water, and then was amplified and inserted into the BglBrick plasmid pE1k (4206 bp) (Jia et al., 2020) using restriction sites *Nde*I/*Bam*HI, resulting in the plasmid pE1k-*GlnRS* (Fig. S1). *E. coli* DH5α was used for cloning and expression of a recombinant plasmid, resulting in *E. coli* DH5α/pE1k-*GlnRS* with overexpression of *GlnRS*. The oligonucleotides used for the construction of plasmids designed by using Primer Premier 5 are listed in Table S1.

2.4. Verification of bacterial phenotype after exposure to chloramine

Single colonies of wild-type *E. coli* DH5α and *E. coli* DH5α/pE1k-*GlnRS* were grown in 5 mL of LB media overnight at 37 °C. The bacteria were washed with fresh M9 media and resuspended to obtain an initial optical density of 0.2 at 600 nm (OD_{600}) due to LB could quench chloramine (Drazic et al., 2015). After bacterial strains grew at 37 °C and 230 rpm for 60 min, they were mixed with chloramine solution at the desired concentration at room temperature for 30 min. The chloramine disinfection reaction was terminated by adding 0.1 M sodium thiosulfate. The growth curve line was monitored in 1 h increments at 600 nm in a Spark enzyme labeling instrument (TECAN, Switzerland). The OD of each biological replicate was averaged (n = 3) for plotting.

Wide-type *E. coli* DH5α and *E. coli* DH5α/pE1k-*GlnRS* strains were used for flow cytometric measurements (FCM). Intact cell concentrations (ICCs) of the two strains were measured after exposure to chloramine solution at the desired concentration. Enumeration of ICC was performed by using SYBR® Green I stain and propidium iodide as described in previous studies (Gillespie et al., 2014). FCM measurements were performed with a CytoFLEX flow cytometer (Beckman Coulter, Inc. USA).

2.5. High-throughput sequencing and shotgun metagenomics sequencing

The enrichment of bacteria in water was performed using membrane filtration and the extraction of genomic DNA from the membrane was performed using an optimized phenol:chloroform-based method as described in our previous studies (Miao and Bai, 2021). DNA quality was checked by 2% agarose gel electrophoresis. Qualified DNA was adjusted to 50 ng/μL and stored at −80 °C.

A total of 160 water samples (Table S2) were used for high-throughput sequencing, including 62 samples in the waterworks, 58 samples in the Primary DWDS (PrimDWDS), and 40 samples in the Secondary DWDS (SecDWDS). The V3–V4 hypervariable regions of the bacterial 16S rRNA gene were amplified with primers 338F and 806R (Mori et al., 2014). Sequencing was performed by Illumina MiSeq technology. The 16S taxonomic alignment was performed against the Silva Seed v138 database (Quast et al., 2013), and putative microbial functions were predicted using Tax4Fun and PICRUSt2 (Yu et al., 2021). The bacterial phenotype was predicted by using BugBase (https://bugbase.cs.umn.edu).

A total of 8 water samples in DWTSs were used for shotgun sequencing, including raw water and effluent water in DWTS #1, BAC water and effluent water in DWTS #2, and raw water, BAC water, UV water and effluent water in DWTS #3. Shotgun sequencing was performed using Illumina HiSeq 2000. NEXTflex™ Rapid DNA-Seq Kit (Bioo Scientific, USA) was used to construct the library. CD-HIT (http://www.bioinformatics.org/cd-hit/), SOAPaligner, and BLASTP were used for abundance calculations of nonredundant gene sets and annotation of the KEGG orthologies and modules (Li et al., 2009a).

2.6. Statistical analysis

All data analyzed in this study were considered statistically significant at $p < 0.05$ unless indicated otherwise. Mothur 1.30.1 was used to estimate the bacterial alpha diversity index (i.e., Richness and Shannon index) (Schloss et al., 2009). Spearman analysis was performed to explore the correlation between gene abundance and bacterial alpha diversity. Partial least squares discriminant analysis (PLS-DA) and nonparametric analysis of Adonis distance matrices were performed to compare bacterial composition among water samples (Warton et al., 2012). Co-occurrence networks of bacterial approaches were created by the "WGCNA" package and "Gephi" (Bastian M., 2009). The abundant features were analyzed by using Scheffe's significant difference test and Wilcoxon rank-sum test (Dixon, 2003).

3. Results and discussion

3.1. CRB composition in the water supply systems

Four types of chlorine-resistant strains were isolated from 39 water samples with a total chlorine concentration higher than 0.5 mg/L in DWDS (Table 1, Table S3). Except for *Mycobacterium*, the other three genera are G⁻ strains. All the above bacteria have been detected in chlorinated DWSSs (Li et al., 2020; Zhang et al., 2018).
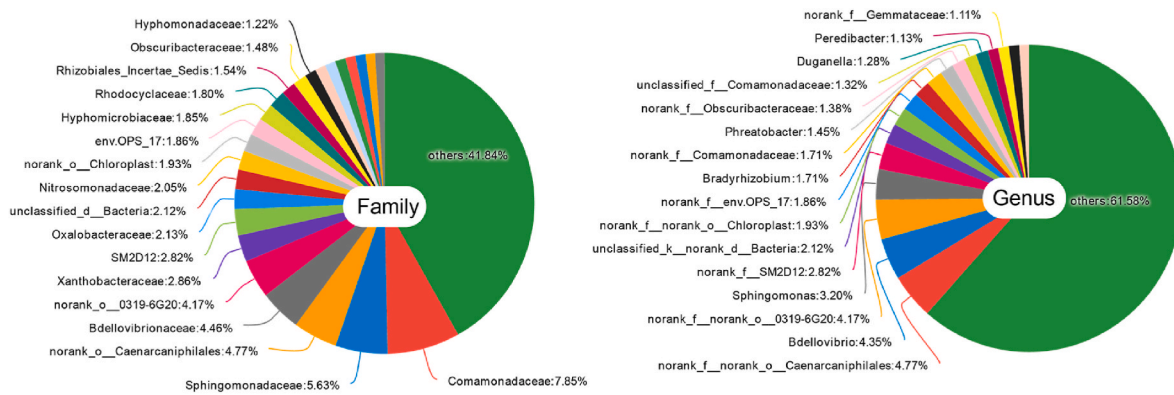
Fig. 2. Percentage of chlorine-resistant bacteria at the family and genus levels in DWSSs by high-throughput sequencing. Others indicate bacteria with a relative abundance less than 1%.
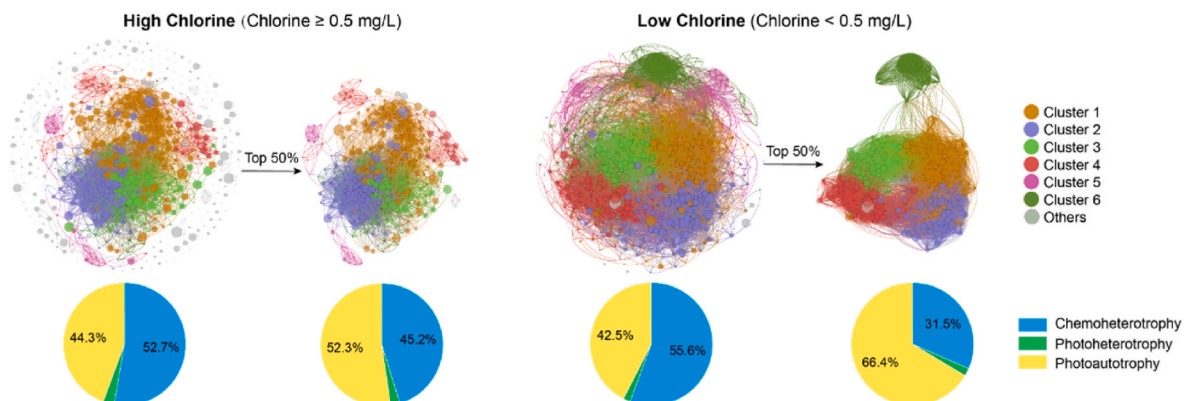
Fig. 3. Whole-community biological networks and bacterial assimilatory types in DWSSs. Networks were colored according to modularity class and order. The size of the nodes was proportioned to the relative abundance of each OTU. The filtered networks were identified as having a high network weighted degree level (top 50%).

Two-thirds of bacteria were found to be in a viable but nonculturable (VBNC) state in DWSSs (Kalmbach et al., 1997). To screen the CRB in the VBNC state, high-throughput sequencing was performed on 160 water samples from DWSSs (Table S2). There were 77 water samples with a total chlorine concentration greater than 0.5 mg/L, including 12 effluent water samples, 53 PrimDWDS samples, and 12 SecDWDS samples. Bacteria in these water samples were regarded as CRB, and the species composition is shown in Fig. 2. Except for the bacteria in Table 1, other nonculturable CRBs were identified by high-throughput sequencing, and the top four genera in relative abundance were *Bdellovibrio*, *Peredibacter*, *Pedomicrobium* and *Hydrogenophaga*. All four bacteria are G⁻ bacteria that have an important impact on human health and sensory indicators for water quality, but their chlorine resistance mechanism has not been studied.

3.2. Co-occurrence patterns of CRB in the water supply systems

Considering the differences in community structure between CRB and non-CRB, the co-occurrence patterns of the two types of bacteria were compared. Two biological correlation networks were constructed based on Spearman's rank correlation coefficient matrix of the relative abundances of 692 bacterial genera (Fig. 3). Networks were colored according to the cluster module, and the node size of the networks was directly proportional to the relative abundance of each genus. The genus composition of bacteria at each node is shown in Fig. S2. The average path length of the CRB network was longer than that of the non-CRB network, so the transmission efficiency of energy and substances among CRB was lower. Specifically, the metabolic efficiency of CRB was lower than that of the non-CRB (Table S4). The average clustering

coefficient of the CRB network was higher than that of the non-CRB network, which suggested that the clustering degree of CRB was high (Table S4).

The top 50% edges of the two networks were selected based on the edge weights (Fig. S3). It was found that the relative abundance of CRB with high interconnection was also high, such as the abovementioned *Bdellovibrio*, *Bradyrhizobium*, *Peredibacter*, *Sphingomonas*, and *Hydrogenophaga* (Table S5). The assimilation of both CRB and non-CRB was dominantly chemotrophic metabolism, which accounted for 52.7% and 55.6% of the total assimilation metabolism, respectively. The chemotrophic metabolism of CRB with high interconnection accounted for 45.2% of the total assimilation metabolism, which was 1.5 times higher than that of non-CRB with high interconnection. Most bacteria obtained energy by chemical heterotrophic metabolism, and the efficiency of photoautotrophic metabolism was low in hermetic DWSSs. The longer the average path length of networks, the lower transmission efficiency of energy and substances, so the lower the metabolic efficiency (Layeghifard et al., 2017; Zhou et al., 2011). The higher the average clustering coefficient of networks, the higher the clustering degree (Guo et al., 2022). Therefore, there is a strong interaction among dominant CRBs at high disinfection doses, which can be used to maintain basic metabolism. Because of the continuous oxidation stress of chloramine, the interaction among all CRBs was sparse, and the metabolic efficiency was low.

3.3. Key metabolic pathways to CRB

A total of 9 bacterial phenotypes of CRB at high chloramine doses and non-CRB at low chloramine doses were compared using the
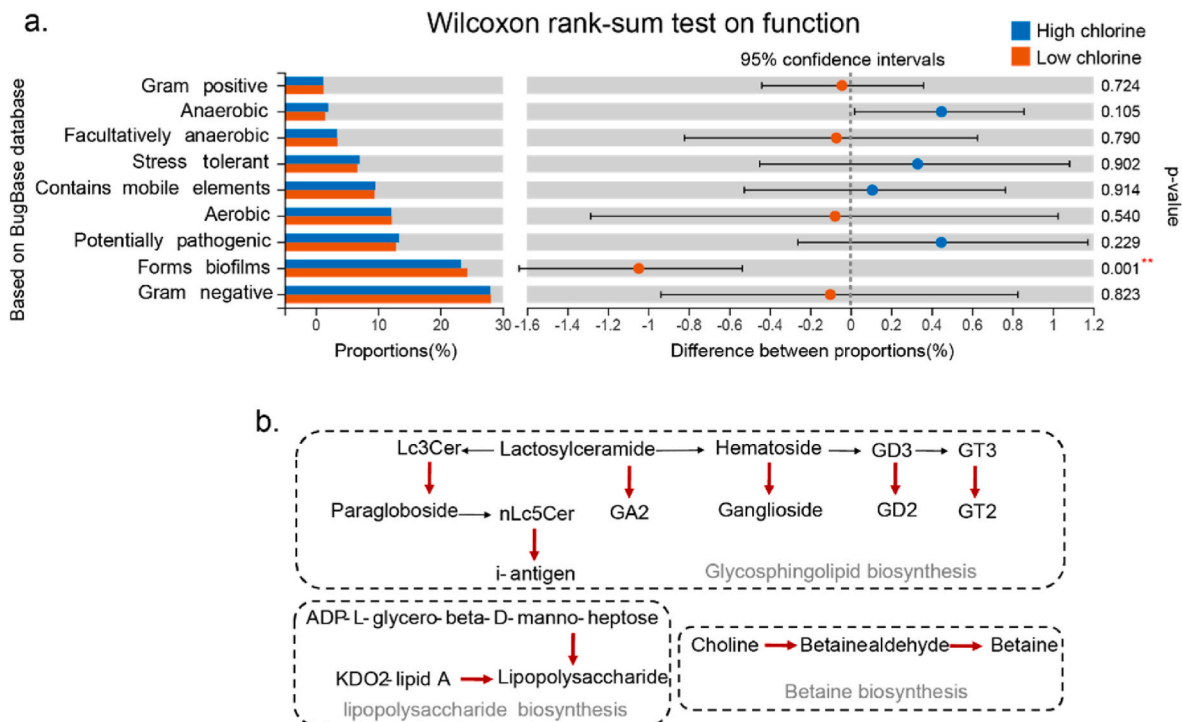
Fig. 4. Bacterial phenotype and function prediction. (a) Wilcoxon rank-sum test of bacterial phenotypes based on the BugBase database between the distinct groups in DWSSs. **(b)** Specific metabolic pathways (red) and the corresponding metabolic modules (gray) of CRB. (For interpretation of the references to color in this figure legend, the reader is referred to the Web version of this article.)

Wilcoxon rank-sum test (Fig. 4a). Because both CRB and non-CRB were mainly G⁻, the chlorine resistance of CRB obtained from external phenotypic factors of the cell wall was limited. The relative abundance of the oxidative stress tolerance phenotype of CRB was higher than that of non-CRB, so the chlorine resistance of CRB may be given by the internal genetic pathway.

By comparing the relative abundance of bacterial metabolic pathways in high (≥ 0.5 mg/L) and low chlorinated water (<0.5 mg/L), some metabolic pathways were found to be key to CRB (Fig. 4b). First, CRB is involved in glycosphingolipid biosynthesis (KEGG M00071 and KEGG M00069). Glycosphingolipids have long been regarded as modulators of cell growth, adhesion, and transmembrane signaling (Mencarelli and Martinez Martinez, 2013). Structurally, glycosphingolipids are formed from hydrophobic ceramide (Cer) skeletons, which can form tightly packed and thick membrane structures, resulting in low permeability of

the plasma membrane to ions and peptides. Therefore, they have a strong barrier function to the extracellular environment (Simon et al., 2021). Glycosphingolipid is also one of the main components of extracellular polymeric substances (EPS), which provide the first barrier for bacteria to prevent chloramine oxidation (Gutman et al., 2014). Second, CRB is involved in lipopolysaccharide biosynthesis (KEGG M00080). Lipopolysaccharide is a highly acylated saccharolipid located on the outer leaflet of the outer membrane of G⁻ bacteria. Lipopolysaccharide is critical to maintaining barrier function and preventing the passive diffusion of hydrophobic solutes such as antibiotics and detergents into the cell (Zhang et al., 2013). Although G⁻ bacteria have no large amount of peptidoglycan protection, the vigorous metabolism of lipopolysaccharide was beneficial to maintain the intact cell wall of G⁻ CRB and formed a second barrier to prevent chloramine oxidation. Third, CRB is involved in betaine biosynthesis (KEGG M00555). Betaine is an
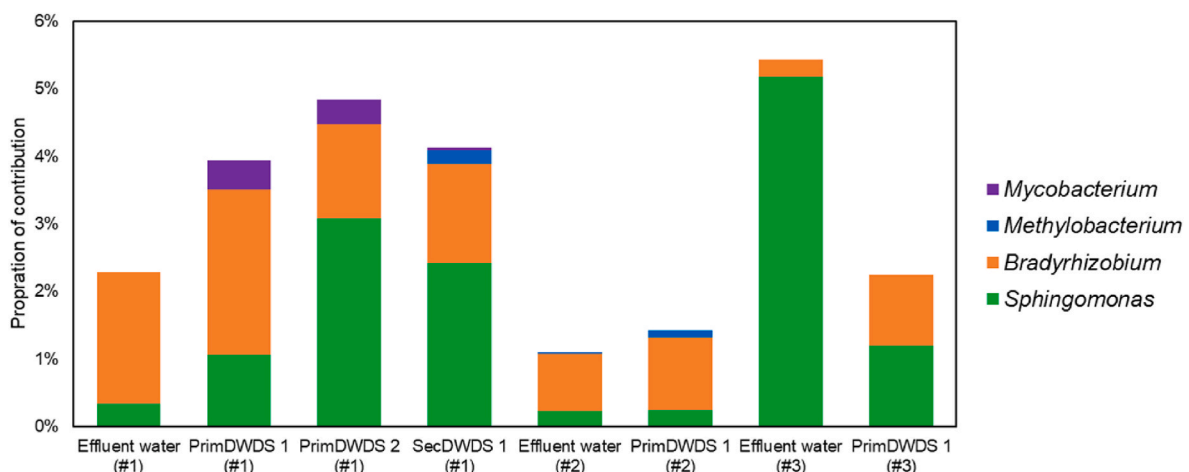
Fig. 5. Contribution of isolated CRBs to *GlnRS* genes by shotgun sequencing.
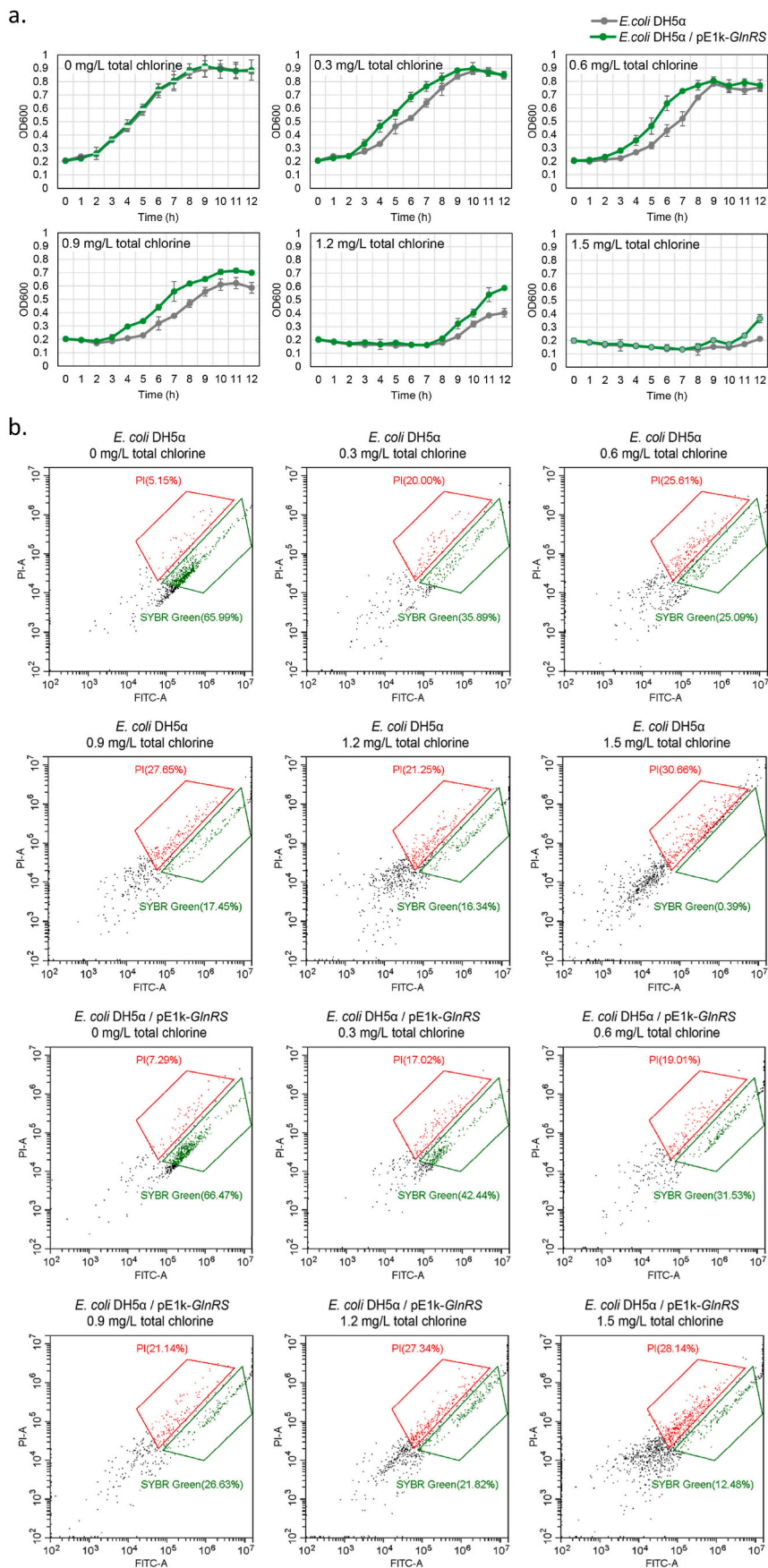
Fig. 6. Comparison of the growth curves (a) and intact cell concentration (b) of wild-type *E. coli* DH5α and *E. coli* DH5α/pE1k-*GlnRS* after exposure to chloramine.

amphoteric compound that can be used as an osmotic regulator to provide normal osmotic pressure to cells, further reducing the impact of chloramine oxidation stress on cells and forming a third barrier to prevent chloramine oxidation (Zou et al., 2016).

Although some metabolic pathways are key and specific to the CRB, they only account for 4.21% of all the metabolic pathways, and 94.08% of metabolic pathways were shared by CRB and other bacteria. By using PICRUSt2 functional prediction based on the IMG database, it was found that the dominant metabolic pathway of CRB was mainly related to translation, which belongs to genetic information processing, including aminoacyl-tRNA biosynthesis and ribosome biogenesis (Table S6). *GlnRS* was the dominant enzyme of CRB (Table S7). The equation of glutaminyl-tRNA biosynthesis is shown in Fig. S4. In addition, by using Tax4Fun functional prediction based on the Silva database, we found the dominance of aminoacyl-tRNA biosynthesis (Table S8) and *GlnRS* (Table S9). Aminoacyl-tRNA biosynthesis, *GlnRS* and glutaminyl-tRNA synthase genes were more dominant after chloramine disinfection using the Wilcoxon rank-sum test. The results of high-throughput sequencing showed that the relative abundance of *GlnRS* and the related orthologous genes increased by 10.11% and 14.58%, respectively, after chloramine disinfection (Table S10). Shotgun sequencing indicated that all the isolated CRB in Table 1 carried *GlnRS* genes (Fig. 5). The relative abundance of *GlnRS* was significantly positively correlated with the bacterial species number and diversity (Table S11). Specifically, the changes in bacterial species number and diversity in DWDSs were synchronized with the expression of *GlnRS* (Table S12). Because high *GlnRS*-expressing bacteria have a stronger protein translation ability, the forced translation of part of damaged bacteria under chloramine stress may lead to an increase in species diversity.

3.4. Effects of GlnRS overexpression on the chloramine resistance of bacteria

The growth curves of wild-type *E. coli* DH5α and *E. coli* DH5α/pE1k-*GlnRS* overexpressing *GlnRS* were compared to characterize the effect of *GlnRS* overexpression on bacterial chloramine resistance (Fig. 6a). In the absence of total chlorine, both types of bacteria reached the exponential phase rapidly. In the presence of 0.3 mg/L, 0.6 mg/L and 0.9 mg/L total chlorine, the growth curves of the bacteria included three phases: lag phase, exponential phase, and stabilization phase. However, decline phases in each growth curve could not be revealed because we only assayed the total numbers of bacteria, including living and dead ones, based on the value of OD600 (Li et al., 2009b). However, when exposed to 1.2 mg/L and 1.5 mg/L total chlorine, *E. coli* lagged to 8 h and 10 h, respectively. With increasing total chlorine concentration, the delay was more evident. The growth of the *GlnRS* overexpression strain was faster than that of the wild-type strain after exposure to chloramine, suggesting that the *GlnRS* overexpression strain had stronger chlorine resistance.

After exposure to 0.3 mg/L, 0.6 mg/L, 0.9 mg/L, 1.2 mg/L, and 1.5 mg/L total chlorine for 30 min, the ICC of wild-type *E. coli* DH5α decreased by 81.05%, 87.24%, 91.17%, 91.31% and 99.76%, respectively, and the average inactivation rate was 90.11% (Fig. 6b). In contrast, the ICC of *E. coli* DH5α/pE1k-*GlnRS* decreased by 62.14%, 81.68%, 83.79%, 86.92% and 92.45%, respectively, after exposure to chloramine, and the average inactivation rate was 81.40% (Fig. 6b). The inactivation rate of the *GlnRS* overexpression strain was lower than that of the wild-type strain after exposure to chloramine, also suggesting that the *GlnRS* overexpression strain had stronger chlorine resistance.

Aminoacyl-tRNA synthetases catalyze one of the most important reactions of the biosphere because they recognize and connect cognate tRNA to its cognate amino acid and form a specific aminoacyl-tRNA (Di Giulio, 2017). The catalytic activities for glycyl-, lysyl-, and tryptophanyl-tRNA synthetase have been adapted to synthesize diadenosine polyphosphates, which are believed to regulate glucose metabolism, cell proliferation, and death (Park et al., 2008). *GlnRS*

belong to the broad class of aminoacyl-tRNA synthetases, which might play an important role in protecting cells from apoptosis induced by different stimuli (Ko et al., 2001; Paravisi et al., 2009).

4. Conclusions

CRB isolated from the DWSSs included *Methylobacterium* (7%), *Sphingomonas* (9%), *Mycobacterium* (24%), and *Bradyrhizobium* (61%). Other uncultured or not easily cultured CRBs included *Bdellovibrio*, *Peredibacter*, *Pedomicrobium*, and *Hydrogenophaga* by high-throughput sequencing. Dominant CRB strongly interacted with each other under high disinfectant stress to maintain basic metabolism. A total of 4.21% of the bacterial metabolic pathways were key and specific to CRB. Glutaminyl-tRNA biosynthesis was the dominant metabolic pathway of CRB. After chloramine disinfection, the relative abundance of *GlnRS* and the related orthologous genes increased by 10.11% and 14.58%, respectively. The inactivation rate of the *GlnRS* overexpression strain (81.40%) was lower than that of the wild-type strain (90.11%) after exposure to chloramine. Meanwhile, the growth rate of the *GlnRS* overexpression strain was higher than that of the wild-type strain. Glutaminyl-tRNA biosynthesis enhanced the chlorine resistance of bacteria in DWSSs. This research brings new insight regarding the intrinsic mechanism for CRB by investigating full-scale DWSSs instead of model strains in the lab. As the internal intrinsic resistance is from the genetic materials, the combined disinfection process of UV and chloramine may help to downregulate the GlnRS gene and hence enhance the effectiveness of chloramine disinfection, especially for the control of chlorine-resistant pathogens in drinking water.

Author statement

Xiaocao Miao: Data curation, Methodology, Visualization, Investigation, Writing - original draft. **Xue Han:** Data curation. **Chenxu Liu**: review and editing. **Xiaohui Bai:** Conceptualization, Methodology, Supervision, Writing - review & editing.

Declaration of competing interest

The authors declare that they have no known competing financial interests or personal relationships that could have appeared to influence the work reported in this paper.

Data availability

Data will be made available on request.

Appendix A. Supplementary data

Supplementary data to this article can be found online at https://doi.org/10.1016/j.chemosphere.2022.136322.

References

Bai, X., Ma, X., Xu, F., Li, J., Zhang, H., Xiao, X., 2015a. The drinking water treatment process as a potential source of affecting the bacterial antibiotic resistance. Sci. Total Environ. 533, 24–31.

Bai, X., Zhi, X., Zhang, M., Zhu, H., Meng, M., 2015b. Real-time ArcGIS and heterotrophic plate count based chloramine disinfectant control in water distribution system. Water Res. 68, 812–820.

Bastian, M., H.S.J.M., 2009. Gephi: an open source software for exploring and manipulating networks. In: International AAAI Conference on Weblogs and Social Media, 8, pp. 361–362.

Bereschenko, L.A., Stams, A.J.M., Euverink, G.J.W., van Loosdrecht, M.C.M., 2010. Biofilm formation on reverse osmosis membranes is initiated and dominated by Sphingomonas spp. Appl. Environ. Microbiol. 76, 2623–2632.

Cloete, T.E., 2003. Resistance mechanisms of bacteria to antimicrobial compounds. Int. Biodeterior. Biodegrad. 51, 277–282.

Cox, C.R., Gilmore, M.S., 2007. Native microbial colonization of Drosophila melanogaster and its use as a model of Enterococcus faecalis pathogenesis. Infect. Immun. 75, 1565–1576.

Demple, B., 1996. Redox signaling and gene control in the Escherichia coli soxRS oxidative stress regulon — a review. Gene 179, 53–57.

Di Giulio, M., 2017. The aminoacyl-tRNA synthetases had only a marginal role in the origin of the organization of the genetic code: evidence in favor of the coevolution theory. J. Theor. Biol. 432, 14–24.

Dixon, P., 2003. VEGAN, a package of R functions for community ecology. J. Veg. Sci. 14, 927–930.

Douterelo, I., Fish, K.E., Boxall, J.B., 2018. Succession of bacterial and fungal communities within biofilms of a chlorinated drinking water distribution system. Water Res. 141, 74–85.

Drazic, A., Kutzner, E., Winter, J., Eisenreich, W., 2015. Metabolic response of Escherichia coli upon treatment with hypochlorite at sub-lethal concentrations. PLoS One 10, e125823.

El-Chakhtoura, J., Prest, E., Saikaly, P., van Loosdrecht, M., Hammes, F., Vrouwenvelder, H., 2015. Dynamics of bacterial communities before and after distribution in a full-scale drinking water network. Water Res. 74, 180–190.

Furuhata, K., Ishizaki, N., Umekawa, N., Nishizima, M., Fukuyama, M., 2014. Pulsed-field gel electrophoresis (PFGE) pattern analysis and chlorine-resistance of Legionella pneumophila isolated from hot spring water samples. Biocontrol Sci. 19, 33–38.

Gillespie, S., Lipphaus, P., Green, J., Parsons, S., Weir, P., Juskowiak, K., Jefferson, B., Jarvis, P., Nocker, A., 2014. Assessing microbiological water quality in drinking water distribution systems with disinfectant residual using flow cytometry. Water Res. 65, 224–234.

Guo, B., Zhang, L., Sun, H., Gao, M., Yu, N., Zhang, Q., Liu, Y., 2022. Microbial co-occurrence network topological properties link with reactor parameters and reveal importance of low-abundance genera. npj Biofilms and Microbiomes 8, 1–13.

Gutman, J., Herzberg, M., Walker, S.L., 2014. Biofouling of reverse osmosis membranes: positively contributing factors ofSphingomonas. Environ. Sci. Technol. 48, 13941–13950.

Jia, X., Zhang, S., Li, J., Xia, J., Yao, R., Zhao, X., Wu, B., Bai, F., Xiao, Y., 2020. Engineered bacterial biofloc formation enhancing phenol removal and cell tolerance. Appl. Microbiol. Biotechnol. 104, 1187–1199.

Kalmbach, S., Manz, W., Szewzyk, U., 1997. Isolation of new bacterial species from drinking water biofilms and proof of their in situ dominance with highly specific 16S rRNA probes. Appl. Environ. Microbiol. 63, 4164–4170.

Ko, Y., Kim, E., Kim, T., Park, H., Park, H., Choi, E., Kim, S., 2001. Glutamine-dependent antiapoptotic interaction of human glutaminyl-tRNA synthetase with apoptosis signal-regulating kinase 1. J. Biol. Chem. 276, 6030–6036.

Langsrud, S., Sidhu, M.S., Heir, E., Holck, A.L., 2003. Bacterial disinfectant resistance—a challenge for the food industry. Int. Biodeterior. Biodegrad. 51, 283–290.

Layeghifard, M., Hwang, D.M., Guttman, D.S., 2017. Disentangling interactions in the microbiome: a network perspective. Trends Microbiol. 25, 217–228.

Li, W., Tan, Q., Zhou, W., Chen, J., Li, Y., Wang, F., Zhang, J., 2020. Impact of substrate material and chlorine/chloramine on the composition and function of a young biofilm microbial community as revealed by high-throughput 16S rRNA sequencing. Chemosphere 242, 125310.

Li, R., Yu, C., Li, Y., Lam, T., Yiu, S., Kristiansen, K., Wang, J., 2009a. SOAP2: an improved ultrafast tool for short read alignment. Bioinformatics 25, 1966–1967.

Li, W., Xie, X., Shi, Q., Zeng, H., Ou-Yang, Y., Chen, Y., 2009b. Antibacterial activity and mechanism of silver nanoparticles on Escherichia coli. Appl. Microbiol. Biotechnol. 85, 1115–1122.

Luo, L., Wu, Y., Yu, T., Wang, Y., Chen, G., Tong, X., Bai, Y., Xu, C., Wang, H., Ikuno, N., Hu, H., 2021. Evaluating method and potential risks of chlorine-resistant bacteria (CRB): a review. Water Res. 188, 116474.

Mencarelli, C., Martinez Martinez, P., 2013. Ceramide function in the brain: when a slight tilt is enough. Cell. Mol. Life Sci. 70, 181–203.

Miao, X., Bai, X., 2021. Characterization of the synergistic relationships between nitrification and microbial regrowth in the chloraminated drinking water supply system. Environ. Res. 199, 111252.

Mir, J., Morató, J., Ribas, F., 1997. Resistance to chlorine of freshwater bacterial strains. J. Appl. Microbiol. 82, 7–18.

Mori, H., Maruyama, F., Kato, H., Toyoda, A., Dozono, A., Ohtsubo, Y., Nagata, Y., Fujiyama, A., Tsuda, M., Kurokawa, K., 2014. Design and experimental application of a novel non-degenerate universal primer set that amplifies prokaryotic 16S rRNA genes with a low possibility to amplify eukaryotic rRNA genes. DNA Res. 21, 217–227.

Ortega Morente, E., Fernández-Fuentes, M.A., Grande Burgos, M.J., Abriouel, H., Pérez Pulido, R., Gálvez, A., 2013. Biocide tolerance in bacteria. Int. J. Food Microbiol. 162, 13–25.

Paravisi, S., Fumagalli, G., Riva, M., Morandi, P., Morosi, R., Konarev, P.V., Petoukhov, M.V., Bernier, S., Chênevert, R., Svergun, D.I., Curti, B., Vanoni, M.A., 2009. Kinetic and mechanistic characterization of Mycobacterium tuberculosis glutamyl-tRNA synthetase and determination of its oligomeric structure in solution. FEBS J. 276, 1398–1417.

Park, S.G., Schimmel, P., Kim, S., 2008. Aminoacyl tRNA synthetases and their connections to disease. Proc. Natl. Acad. Sci. USA 105, 11043–11049.

Quast, C., Pruesse, E., Yilmaz, P., Gerken, J., Schweer, T., Yarza, P., Peplies, J., Glöckner, F.O., 2013. The SILVA ribosomal RNA gene database project: improved data processing and web-based tools. Nucleic Acids Res. 41, D590–D596.

Roy, P.K., Ghosh, M., 2017. Chlorine resistant bacteria isolated from drinking water treatment plants in West Bengal. Desalination Water Treat. 79, 103–107.

Schloss, P.D., Westcott, S.L., Ryabin, T., Hall, J.R., Hartmann, M., Hollister, E.B., Lesniewski, R.A., Oakley, B.B., Parks, D.H., Robinson, C.J., Sahl, J.W., Stres, B., Thallinger, G.G., Van Horn, D.J., Weber, C.F., 2009. Introducing mothur: open-source, platform-independent, community-supported software for describing and comparing microbial communities. Appl. Environ. Microbiol. 75, 7537–7541.

Simões, L.C., Simões, M., Vieira, M.J., 2010. Influence of the diversity of bacterial isolates from drinking water on resistance of biofilms to disinfection. Appl. Environ. Microbiol. 76, 6673–6679.

Simon, M.V., Basu, S.K., Qaladize, B., Grambergs, R., Rotstein, N.P., Mandal, N., 2021. Sphingolipids as critical players in retinal physiology and pathology. J. Lipid Res. 62, 100037.

Warton, D.I., Wright, S.T., Wang, Y., 2012. Distance-based multivariate analyses confound location and dispersion effects. Methods Ecol. Evol. 3, 89–101.

WHO, 2011. Guidelines for Drinking-Water Quality, fourth ed. World Health Organization.

Yu, J., Tang, S.N., Lee, P.K.H., 2021. Microbial communities in full-scale wastewater treatment systems exhibit deterministic assembly processes and functional dependency over time. Environ. Sci. Technol. 55, 5312–5323.

Zhang, G., Meredith, T.C., Kahne, D., 2013. On the essentiality of lipopolysaccharide to Gram-negative bacteria. Curr. Opin. Microbiol. 16, 779–785.

Zhang, J., Li, W., Chen, J., Qi, W., Wang, F., Zhou, Y., 2018. Impact of biofilm formation and detachment on the transmission of bacterial antibiotic resistance in drinking water distribution systems. Chemosphere 203, 368–380.

Zou, H., Chen, N., Shi, M., Xian, H., Song, Y., Liu, J., 2016. The metabolism and biotechnological application of betaine in microorganism. Appl. Microbiol. Biotechnol. 100, 3865–3876.

Zhou, J., Deng, Y., Luo, F., He, Z., Yang, Y., 2011. Phylogenetic molecular ecological network of soil microbial communities in response to elevated CO_2. mBio 2, e00122, 11.